HEI Research Report 240

Predictive, Source-Oriented Modeling and Measurements to Evaluate Community Exposures to Air Pollutants and Noise from Unconventional Oil and Gas Development

Lea Hildebrandt Ruiz et al.

Additional Materials E: Chapter 7

Correspondence may be addressed to Dr. Lea Hildebrandt Ruiz, The University of Texas at Austin, 200 E. Dean Keeton St., Austin, TX 78712; email: lhr@che.utexas.edu.

Although this report was produced with partial funding by the United States Environmental Protection Agency under Contract No. 68HERC19D0010 to the Health Effects Institute, it has not been subjected to the Agency's peer and administrative review and may not reflect the views of the Agency; thus, no official endorsement by the Agency should be inferred. This report also has not been reviewed by private party institutions, including those that support HEI Energy, and may not reflect the views or policies of these parties; thus, no endorsement by them should be inferred.

ACS ES&T Air

Additional Materials E: Chapter 7

pubs.acs.org/estair

Article

Fine Scale Spatial and Temporal Allocation of NOx Emissions from Unconventional Oil and Gas Development Can Result in Increased Predicted Regional Ozone Formation

Mrinali Modi, Yosuke Kimura, Lea Hildebrandt Ruiz, and David T. Allen*

Cite This: ACS EST Air 2025, 2, 130−140

Read Online

ACCESS | Metrics & More | Article Recommendations | Supporting Information

ABSTRACT: The impact of detailed spatial and temporal allocation of unconventional oil and gas development (UOGD) NOx emissions on predicted ozone formation was examined using hydraulic fracturing emissions in the Eagle Ford Shale region of Texas as a case study. Hydraulic fracturing occurs at specific well sites, lasting only 1−2 weeks prior to production. Four scenarios for spatial and temporal allocation of hydraulic fracturing NOx emissions were developed. In one scenario, NOx emissions were evenly distributed to all active wells in the Eagle Ford region, with continuous emissions throughout the year. In other scenarios, NOx emissions from hydraulic fracturing engines in Karnes County were allocated only to fractured wells, with durations ranging from 2 days to 2 weeks. In the month of August, predicted daily maximum of 8 h average (MDA8) O_3 concentrations were consistently 6, 8, and 10 ppb higher over wide regions for the two-week, one-week, and two-day emission periods, respectively, compared to the annual county level distribution, demonstrating that detailed spatial and temporal allocation of NOx emissions in regions like the Eagle Ford Shale, with abundant biogenic VOCs, impacts predicted ozone formation.

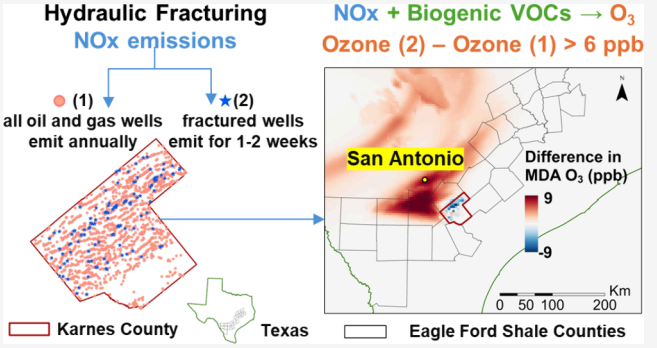

KEYWORDS: *hydraulic fracturing, unconventional oil and gas development, regional ozone, NOx, Eagle Ford*

1. INTRODUCTION

Ground level ozone (O_3) is a greenhouse gas, and a powerful irritant, causing human health effects, vegetation loss and ecosystem damage.[1−3] It is one of six criteria pollutants regulated under the National Ambient Air Quality Standards (NAAQS) by the U.S. Environmental Protection Agency (EPA).[4,5] O_3 in the lower atmosphere (troposphere) is a secondary pollutant, formed from chemical reactions involving nitrogen oxides (NOx) and volatile organic compounds (VOCs) in the presence of sunlight. The formation and accumulation of ozone can be strongly influenced by the spatial and temporal patterns of VOCs and NOx emissions.[6]

In the U.S., unconventional oil and gas development (UOGD) is a rapidly growing source of O_3 precursor emissions. UOGD involves various activities, including exploration, site preparation, drilling, hydraulic fracturing, production, gathering and processing,[7] each of which have diverse sources that contribute to emissions of NOx and VOCs. For example, during the preproduction phase, diesel-powered drilling rigs and flaring can emit both NOx[8] and VOCs.[9] In the production phase, equipment and activities like compressor engines and flaring are known to emit NOx, while majority of VOCs are emitted during routine operations of equipment like condensate, oil, and water tanks, pneumatic controllers and chemical injection pumps.[10] Additionally, other major sources linked with NOx emissions from UOGD include hydraulic fracturing engines and artificial lifts.[8,11] High atmospheric levels of O_3, VOCs, and NOx have been observed in multiple oil and gas producing regions, such as the Northern Front Range in Colorado,[12] the Uintah Basin in Utah,[13] and the Eagle Ford Shale in Texas,[14] among others.[15−17] The proximity of these UOGD regions to major cities has the potential to impact urban air quality and increase NAAQS exceedances of O_3.[18]

The Eagle Ford Shale basin, located in south-central Texas, is one of the most productive oil and gas production regions in the country. In 2022, it ranked third highest in the country for tight oil production (million barrels of oil per day) and fifth highest for shale gas production (billion cubic feet of gas per day).[19,20] This basin is approximately 50 miles in width and

Received: April 3, 2024
Revised: December 15, 2024
Accepted: December 16, 2024
Published: December 30, 2024

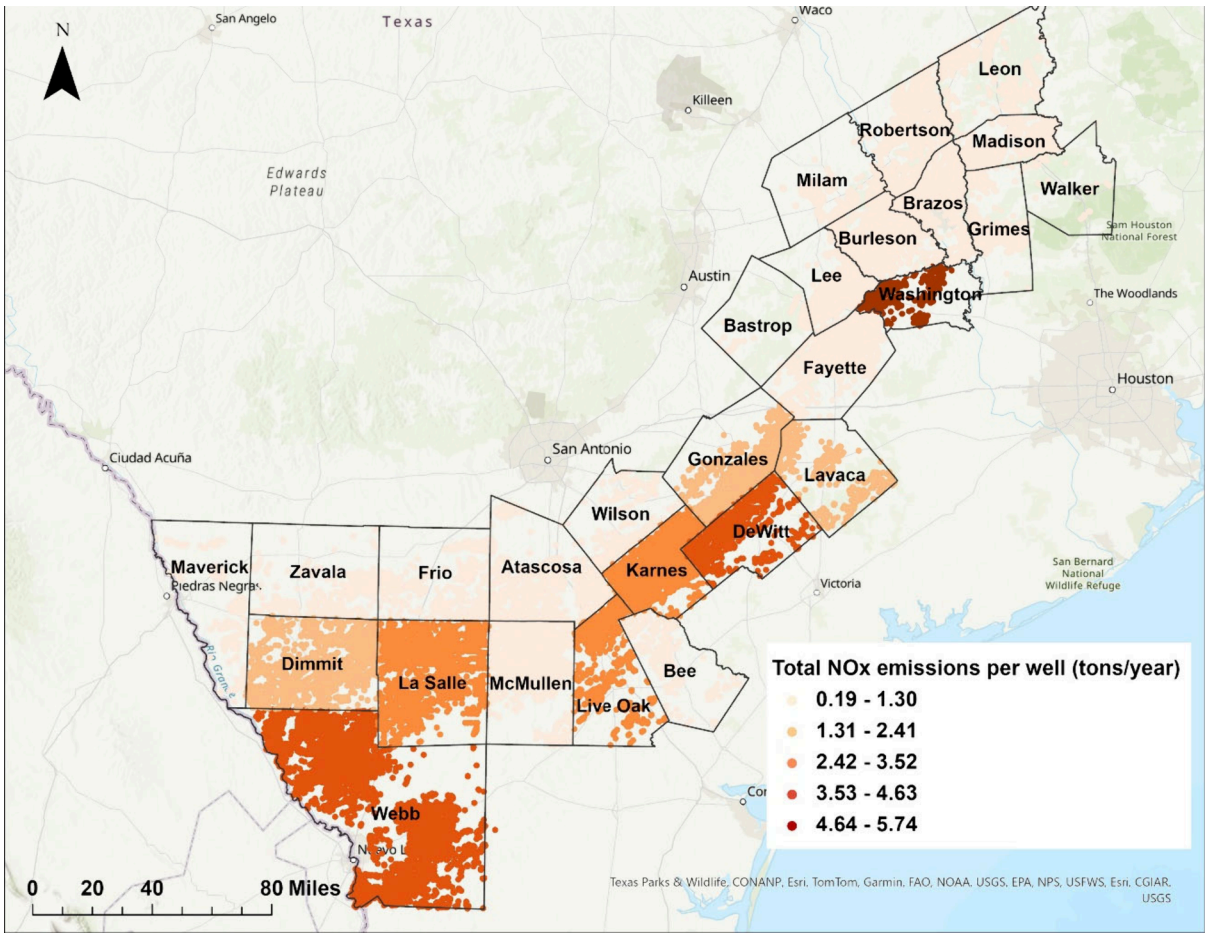

Figure 1. Attributing county-wise TCEQ total NOx emissions spatially to the all the active oil and gas wells in the 27 Eagle Ford Shale counties (Basemap source: Texas Parks and Wildlife).

400 miles in length, spanning 27 Texas counties.[21] San Antonio, the seventh most populous city in the United States,[22] is located north of some of the most active regions of the Eagle Ford Shale and prevailing meteorological conditions frequently advect photochemically aged air from the Eagle Ford Shale into San Antonio,[23] which now exceeds the NAAQS for ozone.[24]

An additional feature of the Eagle Ford region is the high emissions of reactive VOCs from biogenic sources. Isoprene emission rates are particularly high,[25,26] creating atmospheric conditions that are NOx-limited for ozone formation.[23,27] Consequently, emissions of NOx from UOGD in this region have the potential to drive significant ozone formation and accumulation, and the extent of ozone formation and accumulation from UOGD is dependent on the spatial and temporal distributions of the NOx emissions.

Several modeling studies have investigated the impact of increased natural gas production, preproduction activities, and related emissions on regional ozone;[28−30] however, there has been limited emphasis on the detailed spatial and temporal allocation of these emissions. This is because most regional and national emission inventories, such as the National Emissions Inventory (NEI),[31] report NOx and VOC emissions annually with varying spatial resolution. However, some emissions from oil and gas sources are known to have significant spatial and temporal variation, depending on the source and the life cycle of the well.[10] For example, the two major sources of NOx from UOGD are natural gas-fired compressor engines and hydraulic fracturing engines,[32] which have very different emission characteristics. Compressor engines are operated in various stages of a well's life cycle, including exploration, production, processing, and transportation of oil and gas. They are distributed broadly throughout oil and gas production regions and operate both in near continuous mode and intermittently based on demand.[33] Hydraulic fracturing engines, in contrast, are only operational for about 1−2 weeks[34−38] before a well goes into production and only occur at sites where a well is being actively fractured. A lack of accurate spatial and temporal allocation of NOx emissions, particularly for highly localized and episodic sources, such as hydraulic fracturing, in a NOx-limited region like the Eagle Ford Shale, can lead to inaccurate predictions of ozone formation and accumulation, and these uncertainties can influence how ozone mitigation strategies are evaluated.

This work examines the importance of detailed spatial and temporal allocation of NOx emissions from UOGD sources in the Eagle Ford Shale, using NOx emissions from hydraulic fracturing as a case study. Hydraulic fracturing is chosen because it is among the top contributors of NOx emissions in the Eagle Ford Shale. Hydraulic fracturing emissions are localized at wells that are actively being fractured, which typically means that at any given time, only a small number of the tens of thousands of wells in the Eagle Ford Shale have

https://doi.org/10.1021/acsestair.4c00077
ACS EST Air 2025, 2, 130−140

Table 1. Estimating the Emission End Date for Two Fractured Wells, A and B, with Completion Dates of May 25, 2019, and January 8, 2019, Respectively, for Cases 2−4[a]

well	case	emission duration (days)	completion date (emission end date)	estimated emission start date
well A	case 2	14	May 25, 2019, 12:00 AM	May 11, 2019, 12:00 AM
	case 3	7		May 18, 2019, 12:00 AM
	case 4	2		May 23, 2019, 12:00 AM
well B	case 2	14	January 8, 2019, 12:00 AM	December 25, 2018, 12:00 AM
	case 3	7		January 1, 2019, 12:00 AM
	case 4	2		January 6, 2019, 12:00 AM

[a]For Case 1, it was assumed that these wells were emitting continuously throughout the year.

fracturing emissions. Moreover, the duration of fracturing activity is relatively short, lasting from a few days to a few weeks, depending on the specific well.[34−38] The impact of NOx emissions from hydraulic fracturing engines is examined in Karnes County because it has the highest number of drilling permits issued[39] and oil production[40] in the Eagle Ford in recent years. Karnes county is also frequently upwind of San Antonio, and emissions from UOGD in this region have implications for air quality in San Antonio and Bexar County, an ozone nonattainment region.[24]

2. MATERIALS AND METHODS

Emission Scenarios. *Base Case Emissions.* The Base Case emissions used in this work are derived from the 2019 Base Case emission inventory, V1, developed by the Texas Commission for Environment Quality (TCEQ) for use in photochemical modeling.[41] The 2019 Base Case is a part of the modeling platform developed by TCEQ, to support revisions in the State Implementation Plan (SIP) for Bexar County, Dallas-Fort Worth (DFW), and Houston-Brazoria Galveston (HGB) 2015 8 h ozone NAAQS nonattainment areas. In this work, NOx (NO and NO_2) emissions from oil and gas sources for the 27 Eagle Ford Shale counties were removed from the 2019 Base Case and substituted with spatially and temporally resolved NOx emissions to create Cases 1−4, as described below.

Spatially and Temporally Resolved NOx Emissions. For the state of Texas, TCEQ's 2019 Base Case inventory reported ∼235 tons per day (tpd, 85800 tpy) of NOx emissions from oil and gas sources in the Eagle Ford Shale counties for the year 2019 (Table S1 of the Supporting Information, SI). These emissions were reported at the county level for about 47 oil and gas source categories. Tables S2 and S4 of the SI identify the top seven sources of NOx emissions from oil and gas sources within the Eagle Ford Shale counties from the inventory. The remaining sources were labeled as "Others". In 2019, NOx emissions from hydraulic fracturing were estimated to be ∼23.22 tons per day, contributing to about 10% of the total NOx emissions from oil and gas sources in the Eagle Ford Shale (Table S2). Cases 1−4 described below were used to allocate NOx emissions from hydraulic fracturing at various temporal and spatial scales.

In Case 1, the county-level TCEQ total NOx emissions, irrespective of their source, were evenly distributed to all producing wells (active wells) within each county of the Eagle Ford Shale. It was assumed that these wells emit NOx continuously. In 2019, there were 42038 oil and gas producing wells spread across the 27 Eagle Ford Shale counties. The emission rate per well in a county was calculated by dividing the TCEQ total NOx emissions for each county (tpy) by the number of active wells in that county. For example, in Karnes County, in the year 2019, the TCEQ total NOx emissions were approximately 35.3 tpd for a summer day (Table S1) and the total number of active wells was 4185 (Table S3). When these emissions were distributed evenly across all of the wells in Karnes County, total NOx emissions per well became 0.008 tpd or 3.07 tpy. Similar calculations were performed for all the other Eagle Ford Shale counties to obtain a total NOx emission rate per well for each county, using the county's TCEQ total NOx emissions (Table S1) and the number of active wells (Table S3) reported for the year 2019. Figure 1 shows the allocation of the TCEQ total NOx emissions (in tpy per well) to all wells within the Eagle Ford Shale counties, as allocated in Case 1.

In Case 2, TCEQ NOx emissions from hydraulic fracturing engines in Karnes County were allocated only to wells that were fractured in the year 2019. The allocation of all other NOx emissions in Karnes County and in all other Eagle Ford Shale counties was the same as that of Case 1. Additionally, it was assumed that the NOx emissions from hydraulic fracturing were continuous but lasted only for a period of 2 weeks before a well went into production. For example, if a well "A" was completed (ready to produce oil or gas) on May 25, 2019, then the emission duration of the well was allocated to the period from May 11 (12 AM) to May 25 (12 AM), 2019 (Table 1).

The completion dates of wells were obtained from the Railroad Commission (RRC) of Texas's Completion Query system[42] and were utilized to estimate the hydraulic fracturing emission start date and end date. A well completion date marks the completion of the physical construction of a well, and at this stage, it is ready to begin the production of oil or gas. The fractured wells chosen in this work had their completion dates between January 1, 2019, and December 31, 2019.

In 2019, 436 wells were fractured in Karnes County[42] with TCEQ reported NOx emissions of 1958 tpy from hydraulic fracturing (∼5.36 tpd, Table S4). When distributed evenly among the fractured wells, the emission rate becomes 4.5 tons per fractured well. This rate can be further divided by the duration of the hydraulic fracturing event to get the hourly emission rate.

For Cases 3 and 4, the spatial allocation was kept the same as Case 2 but the duration of NOx emissions from hydraulic fracturing was reduced to 1 week and 2 days, respectively. So, for the same well "A", in Cases 3 and 4, the emission period became May 18−25, 2019, and May 23−25, 2019, respectively (Table 1). Emissions were assumed to be continuous during these periods. Case 1 examined the impact of treating total NOx emissions as continuous emissions distributed evenly across all producing wells. Cases 2, 3, and 4, in contrast, examined the impact of changed spatial and temporal distribution of NOx emissions from hydraulic fracturing

https://doi.org/10.1021/acsestair.4c00077
ACS EST Air 2025, 2, 130−140

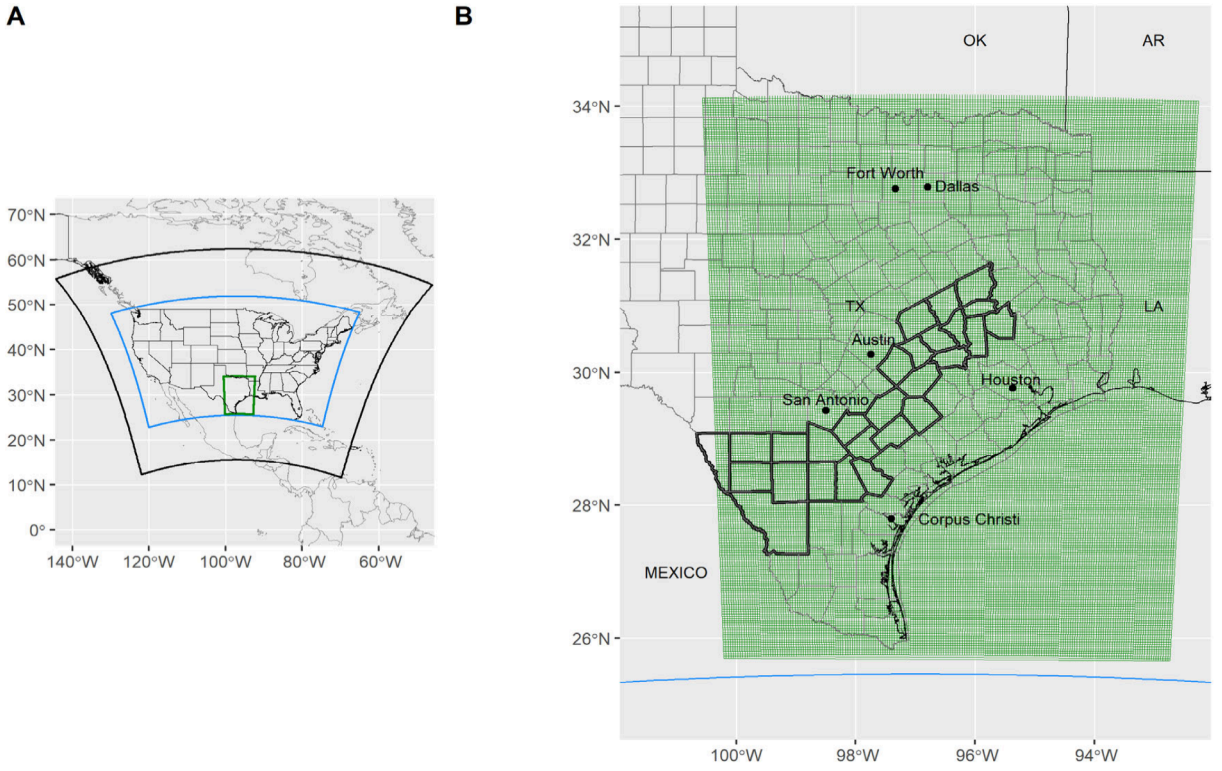

Figure 2. (A) CAMx Modeling domains used in this work. The black and blue boundaries are the nested regional/urban scale 36 and 12 km gridded domains over the United States, respectively. The green region is the nested 4 km gridded domain, covering central and eastern Texas. (B) The 4 km CAMx Modeling Domain. The black regions within are the counties affected by the Eagle Ford Shale basin, located in south-central Texas. The locations of several Texas cities and neighboring regions (black text) are provided for orientation.

engines solely in Karnes County. All other emissions were kept the same as in Case 1.

Photochemical Modeling. The TCEQ total NOx emissions estimated in Cases 1−4 were processed in the Emissions Processing System version3 (EPS3)[43] to generate emission input files for photochemical modeling. The Comprehensive Air Quality Model with Extensions (CAMx, version7.10)[44] was utilized to simulate O_3 impacts from Cases 1−4 and the 2019 Base Case. EPS3 converts the emissions inventory into CAMx ready, speciated (90% NOx by mass is speciated as NO and 10% as NO_2), and spatiotemporally allocated input files. The modeling domains used in this work were nested regional 36/12/4 km grids (Figure 2A). The 36 and 12 km gridded domains covered the entire United States, whereas the 4 km gridded domain covered central and eastern Texas, along with regions of neighboring states from north and east (Louisiana, Oklahoma, and Arkansas), and parts of Mexico from south (Figure 2B). The meteorological episode selected for this work was from April 1 to October 31, 2019. The CAMx modeling grid and the meteorological episode used in this work have been used by TCEQ to evaluate the level of O_3 and regional haze in Texas. Detailed description of model configurations and Base Case model performance evaluation is available at TCEQ's modeling platform.[41]

Metrics for Evaluating O_3. Four metrics were considered to evaluate the impacts of spatially and temporally allocated NOx emissions on regional O_3 formation. The current level of NAAQS for O_3 is set at 70 ppb. The level is calculated as a 3-year average of the annual fourth-highest daily maximum 8 h average O_3 concentrations.[45] Metrics used in this work were based on both 1 and 8 h averaged O_3 concentrations, as predicted by CAMx. The 8 h average O_3 concentration at any hour "h" was calculated by averaging the hourly ozone concentrations from hours "h-7" to "h". These four metrics included the daily maximum of 8 h averaged O_3 concentration at each grid cell (MDA8 O_3), total geographic area exceeding a threshold 8 h average O_3 concentration, time-integrated total geographic area exceeding a threshold 8 h average O_3 concentration and 1 h O_3 concentrations for each grid in the entire domain 4 km domain. The threshold chosen for this work was 60 ppb. The equations below demonstrate how the metrics were calculated.

i. Daily Maximum of 8 h Average (MDA8) O_3 Concentration (ppb) at Each Grid Cell g.

$$\mathrm{MDA8}_g = \max(C_{g8-h,h})$$

$$C_{g8\text{-}h,h} = \{C_{g8\text{-}h,1}, C_{g8\text{-}h,2}, \ldots, C_{g8\text{-}h,24}\}$$

where $C_{g8\text{-}h}$ is the 8 h averaged modeled O_3 concentration (in ppb) in grid cell g at hour h and MDA8 $_g$ is the maximum of 8 h average O_3 concentration (in ppb) in grid cell g for that day.

This metric was calculated for all grid cells in the domain during each episode day. The domain-wide maximum, i.e., highest of the MDA8 O_3 values, was also calculated for each grid cell to examine periods of maximum impacts.

ii. Total Geographic Area Exceeding a Threshold MDA O_3 Concentration of 60 ppbV.

$$\text{area, } A(\mathrm{km}^2) = \Sigma_g a_g\{\delta_g\}$$

where a_g is the area of the grid cell g ($16\ \mathrm{km}^2$)

https://doi.org/10.1021/acsestair.4c00077
ACS EST Air 2025, 2, 130−140

Table 2. Allocation and Estimation of TCEQ Total NOx Emissions from Hydraulic Fracturing in Karnes County per Well (in Tons per Day) for Cases 1−4

cases	nature of NOx emissions from hydraulic fracturing	NOx emissions from hydraulic fracturing allocated in Karnes County[a,b] (tons/year)	No. of wells with allocated emissions[a,b]	NOx emissions per well (tons/event)	emission duration (days)	emission per well (tpd)
case 1	continuous and annual	1958[a]	4185[a]	0.47	365	0.001
case 2	continuous for 2 weeks	1936[b]	436[b]	4.44	14	0.3
case 3	continuous for 1 week	1948[b]		4.47	7	0.6
case 4	continuous for 2 days	1958[b]		4.49	2	2.20

[a]Note that for Case 1, total NOx emissions were allocated to all active wells within the 27 Eagle Ford Shale counties. Within Case 1, NOx emissions from hydraulic fracturing (shown above) were allocated to all wells in Karnes County. [b]For Cases 2−4, NOx emissions from hydraulic fracturing were allocated only to wells fractured in Karnes County in the year 2019, while keeping all other NOx emissions in all counties the same as Case 1.

$$\delta_g = \begin{cases} 1, & \text{MDA8}_g > 60 \\ 0, & \text{MDA8}_g \le 60 \end{cases}$$

This metric examined the MDA8 O_3 concentrations at each grid cell for each episode day and determined if the grid cell exceeded the threshold MDA8 O_3 concentration of 60 ppbV. If the threshold was exceeded for any grid cell, its area was added to the area of exceedance for that day. This metric considered the spatial extent of the ozone exceedance.

iii. Time Integrated Total Geographic Area Exceeding a Threshold 8 h Averaged O_3 Concentration of 60 ppbV.

$$\text{time-integrated area, } A_T(\text{km}^2) = \Sigma_h \Sigma_g a_g(\delta_{g,h})$$

where a_g is the area of the grid cell g (16 km^2)

$$\delta_{g,h} = \begin{cases} 1, & C_{g8\text{-}h,h} > 60 \\ 0, & C_{g8\text{-}h,h} \le 60 \end{cases}$$

This metric examined the 8 h averaged O_3 concentrations at each grid cell for every hour and determined if the grid cell exceeded the threshold 8 h averaged O_3 concentration of 60 ppbV. The areas of all cells exceeding the threshold were then summed for each hour and then for each day. This metric considered both the temporal and spatial extents of ozone exceedance.

iv. One Hour O_3 Concentrations (ppb) at Each Grid Cell g for Every Hour, $C_{g1\text{-}h,h}$. This metric considered the hourly variation in the modeled O_3 concentrations (ppb). Hourly O_3 concentrations at the grid cell nearest to one of the Continuous Ambient Monitoring Station (CAMS 0023) at San Antonio[46] were extracted to understand and compare the localized ozone formation.

3. RESULTS AND DISCUSSIONS

Allocation and Estimation of NOx Emissions. Case 1 distributed the TCEQ total NOx emissions evenly in each of the Eagle Ford Shale counties, such that within a county each well emitted the same amount of NOx emissions. Cases 2−4 performed adjustments in Karnes County and distributed NOx emissions from hydraulic fracturing in Karnes County only to fractured wells in the county. All other NOx emissions within Karnes County, as well as the TCEQ total NOx emissions in all other counties, were kept the same as Case 1.

In Case 1, where NOx emissions from hydraulic fracturing in Karnes County were distributed evenly among all 4185 oil and gas wells in Karnes County, the hydraulic fracturing emissions per well were 0.47 tons. These emissions per well were further reduced to 0.001 tons/day when they were allocated evenly throughout the year (Table 2). For Cases 2−4, NOx emissions from hydraulic fracturing were spatially allocated only to 436 fractured wells, significantly increasing the emissions per well to 4.44 tons. The temporal allocation in Cases 2−4, reduced the emission duration and made NOx emissions from a fractured well more concentrated. As a result, NOx emission rate from hydraulic fracturing (in tons/day) for a well in Case 1 was approximately 300 times lower than Case 2, 600 times lower than Case 3, and 2200 times lower than Case 4, where emissions were localized and episodic, allocated only to fractured wells for a period of 2 days to 2 weeks.

Since at a given time only a small percentage of the total wells have fracturing emissions, lasting for 2 days to 2 weeks, different spatial and temporal distributions of NOx emissions from hydraulic fracturing can lead to NOx emission rates for specific wells at specific times that vary by 3 orders of magnitude. Given the significant variation in NOx emission rates, spanning 3 orders of magnitude, accurately predicting the spatial distribution and magnitude of ozone formation may require detailed spatial and temporal allocation of fracturing emissions.

In Table 2 there are slight differences in TCEQ total NOx emissions from hydraulic fracturing allocated in Karnes County between Cases 1−4. These differences arise because the completion dates of some of the fractured wells were close to the year start date (Jan 1,2019). Consequently, their fracturing emission events did not fall entirely within 2019, leading to slightly differing total emissions depending on the assumed duration of the fracturing. For example, consider Well "B" (Table 1), with a reported completion date of January 8, 2019, 12 AM. In Case 3, where fracturing emissions last for 7 days, the entire emission event falls within the year 2019. However, in Case 2, with a 14-day emission duration, only half of the emission event falls within the year 2019, due to its commencement prior to January 1, 2019 (Table 2). As a result, only half of the emissions from "Well B" were allocated to 2019. Similarly, when fracturing emissions have a duration of 2 days (Case 4), the entire emission event again falls within the year. This contrasts with Well "A", which had a completion date of May 25, 2019, where fracturing emissions for all the Cases fell entirely within the year 2019.

Impact on Regional Ozone Concentrations. To assess the impacts of spatially and temporally allocated NOx emissions on regional ozone, the daily maximum of 8 h average O_3 concentrations (MDA8 O_3) were calculated for each grid cell within the domain on every episode day for Cases 1−4. Using Case 1 as the baseline scenario, the differences in MDA8 O_3 were computed for three spatially

https://doi.org/10.1021/acsestair.4c00077
ACS EST Air 2025, 2, 130−140

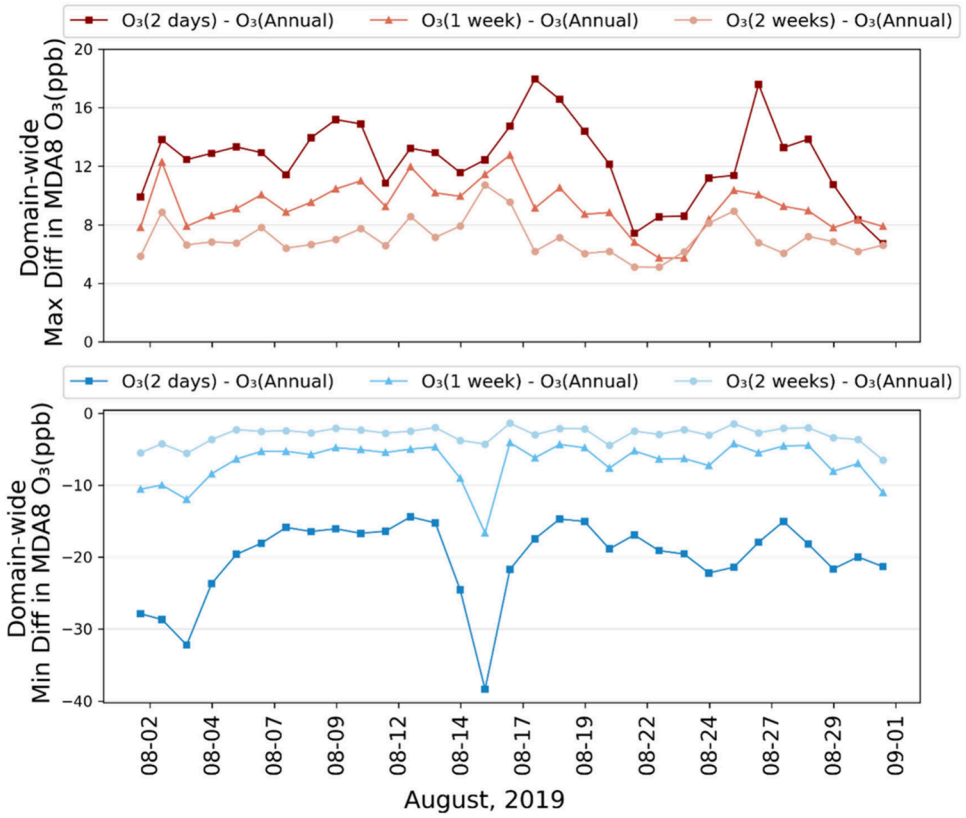

Figure 3. Maximum and minimum differences in domain wide daily maximum of 8 h average O_3 concentrations (MDA8 O_3) between Cases 2−4 and Case 1 (Annual) for August 2019.

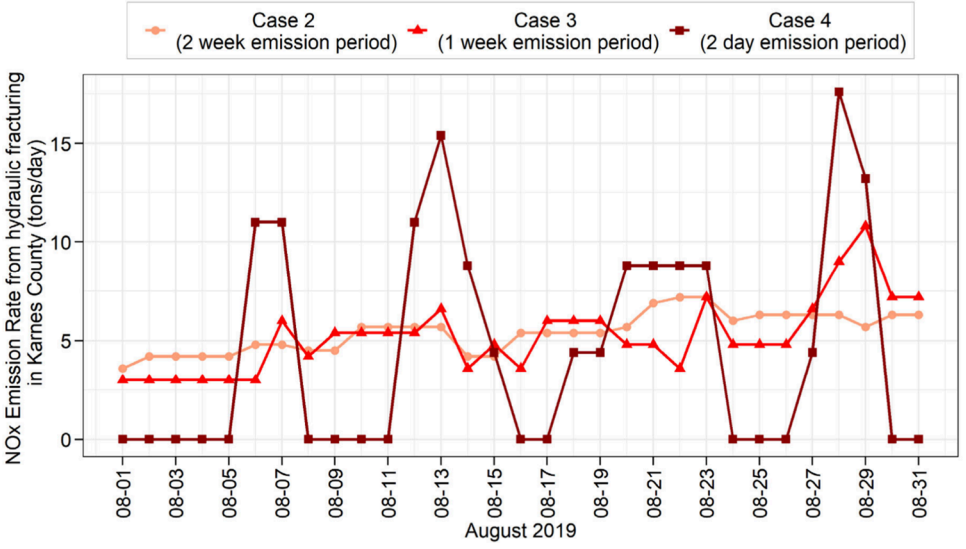

Figure 4. Daily NOx emission rate (tons per day) from hydraulic fracturing in Karnes County for Cases 2−4 in August 2019.

paired scenarios: Case 2−Case 1, Case 3−Case 1, and Case 4−Case 1. This was done for each grid cell and for each episode day. The maximum and minimum differences in MDA8 O_3 concentrations were then identified across the domain for each of the three paired scenarios for each episode day. This process resulted in two values (maximum and minimum differences) across the domain for each episode day. These values were used to identify "high impact periods", the days or months when the most significant positive and negative impacts on MDA8 O_3 concentrations occur relative to Case 1, due to difference in NOx allocation.

As the emission duration decreased from Cases 1 to 4 (Table 2), significant changes were observed in the domain wide MDA8 O_3 concentrations throughout the entire episode. One of the high impact periods was the month of August (Figure 3), where the domain-wide maximum MDA8 O_3 concentrations were consistently 6, 8, and 10 ppb higher than the annual distribution (Case 1) for the two-week, one-week, and two-day emission period, respectively. Similar

https://doi.org/10.1021/acsestair.4c00077
ACS EST Air 2025, 2, 130−140

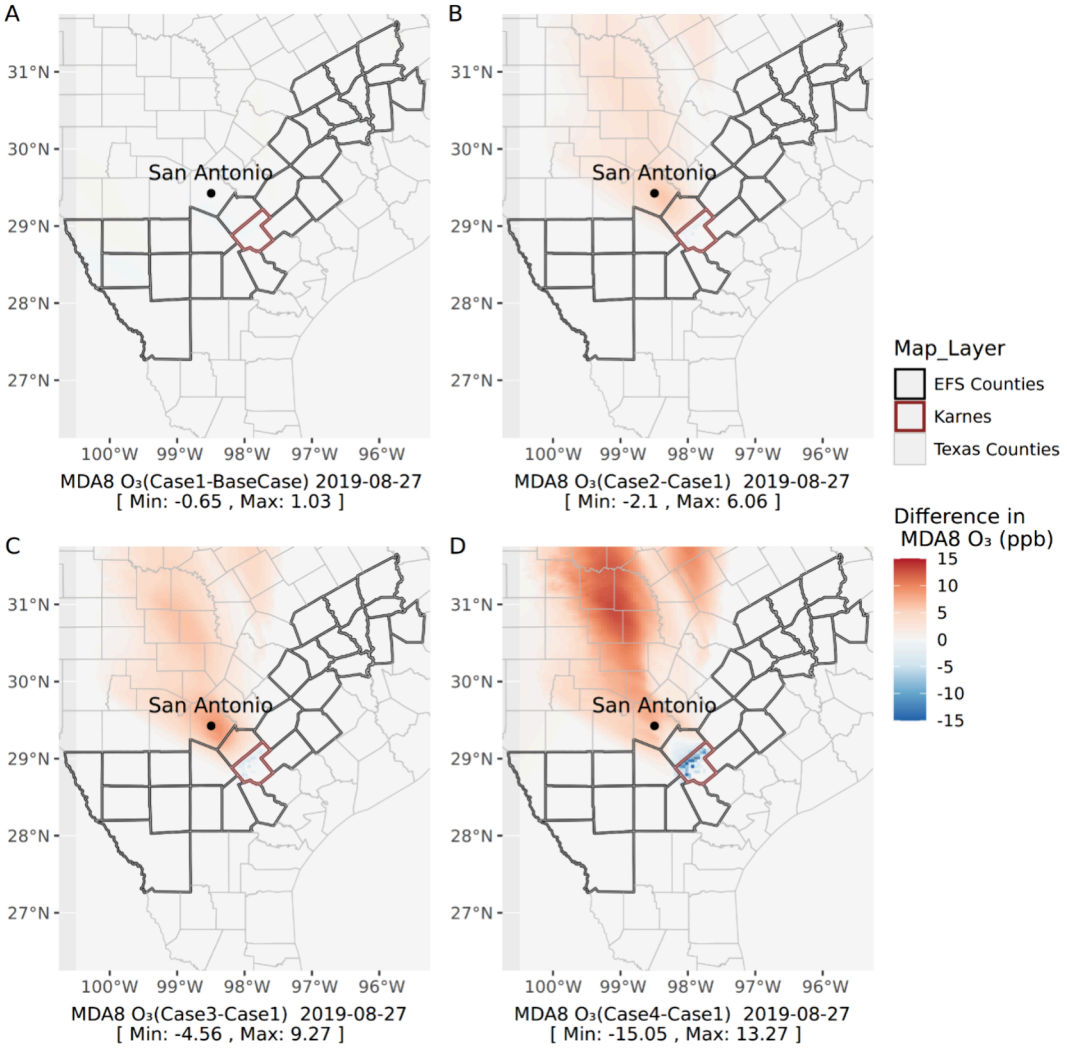

Figure 5. Differences in the daily maximum of 8 h average (MDA8) O_3 concentrations between Case 1 and Base Case (A) and Cases 2−4 and Case 1 (B−D) on August 27, 2019. Counties outlined in black are counties in the Eagle Ford Shale basin; the counties outlined in red are Karnes County.

behavior was also observed during most of July and September (Figures S1 and S2). Moreover, there were at least 2 days in every month from June to August where MDA8 O_3 concentrations were 9, 12, and 16 ppb higher than the annual distribution for the two-week, one-week, and two-day emission period, respectively.

When hydraulic fracturing emissions were concentrated in time and space (Cases 2−4), regions with high NOx emissions experienced prompt reactions between NO and ozone, forming NO_2 and thus reducing the local concentration of O_3 concentrations. This explains the decreasing MDA8 O_3 concentrations and increasing negative differences in MDA8 O_3 concentrations from Case 4 to Case 2 (Figure 3). With regional transport, NO_2 can travel downwind and further react in the atmosphere, contributing to more ozone formation away from the emission sources. This process leads to higher ozone concentrations in downwind areas, explaining why higher MDA8 O_3 concentrations were observed in Cases 2−4 compared to Case 1.

Case 4 showed the largest variability between the maximum and minimum MDA8 O_3 concentrations on any given day. This can be attributed to the highly concentrated NOx emissions from hydraulic fracturing, which led to a highly variable temporal distribution of these emissions in August. Figure 4 shows the daily NOx emission rate (tons per day) from hydraulic fracturing in Karnes County for Cases 2−4 in August 2019. In Case 4, while some days in August had zero NOx emissions from hydraulic fracturing, others have almost 3−5 times more emissions compared to Cases 2 and 3. Due to the complex chemistry and regional transport of ozone, it is not surprising that, despite some days having lower NOx emissions in Karnes County for Case 4 compared to Cases 2 and 3, higher ozone levels are observed in other parts of the domain, regardless of the low or zero NOx emissions in Karnes County.

Case 2, with a 2-week emission period, exhibited the least day to day variability in domain-wide MDA8 O_3 differences among the three cases. This is expected because the relatively longer emission period results in less variability in NOx emissions over time (Figure 4), leading to smaller maxima and minima in MDA8 O_3 concentrations compared with Cases 3 and 4. Finally, Case 3, with a 1 week emission period, shows more variability in NOx emission rates than Case 2 but less than Case 4, resulting in positive and negative differences in domain-wide MDA8 O_3 that are more pronounced than in Case 2 but less so than in Case 4 (Figure 3). Figures S4 and S5

https://doi.org/10.1021/acsestair.4c00077
ACS EST Air 2025, 2, 130−140

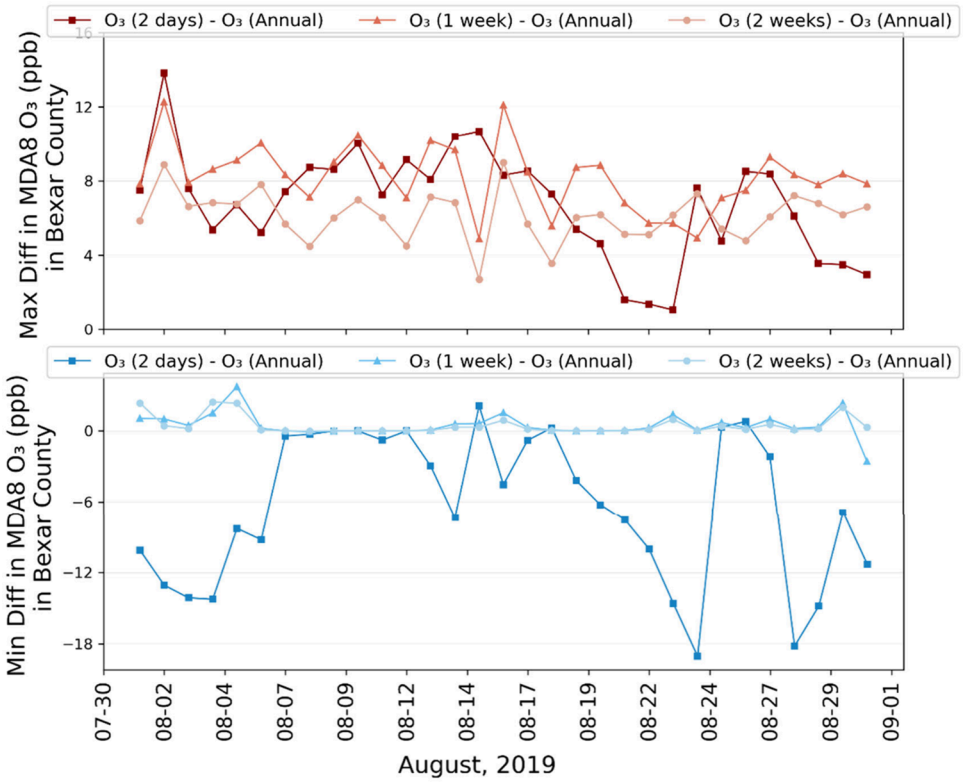

Figure 6. Maximum and minimum differences in the daily maximum of 8 h average O_3 concentrations (MDA8 O_3) between Cases 2−4 and Case 1 (Annual) in Bexar County for August 2019.

of the SI show the daily variability in the NOx emission rate (tons per day) from hydraulic fracturing along with the number of wells undergoing fracturing in Karnes County in August 2019 for Cases 2−4.

Due to persistent high MDA8 O_3 enhancements, the month of August was selected to further understand thespatial distributions of ozone enhancements. Figure 5B−D shows the differences in MDA8 O_3 concentrations between Case 1 and Cases 2−4 for the entire domain on a high impact day in August. Due to the high NOx emission rates in Cases 2−4 (Table 2), ozone has a prompt reaction with NO to form NO_2, in the regions with spatially and temporally concentrated NOx sources (here Karnes County), leading to lower MDA8 O_3 concentrations (blue shaded region in Figure 5) than Case 1. However, with regional transport, NO_2 reacts further, leading to higher net ozone formation in areas such as San Antonio and nearby regions of Bexar County (red regions in Figure 5) than Case 1. There were several days in August that showed analogous behavior. These results suggest that NOx emissions from hydraulic fracturing, if accurately allocated, can lead to increased predicted MDA8 O_3 concentrations, with enhancements ranging from 1 to 10 ppb in the areas surrounding the Eagle Ford Shale. Figure 5A shows the differences in MDA8 O_3 concentrations between TCEQ 2019 Base Case and Case 1 for the same day which are less than 1 ppb.

Hydraulic fracturing typically takes place over a period of 4−8+ days, depending on the size and complexity of the well.[34−38] So, Case 3, with an emission duration of 1-week, is the most likely representation of NOx emissions from hydraulic fracturing engines. Figure S3 shows the differences in the daily maximum of 8 h average MDA8 O_3 concentrations between Case 1 and Case 3 for several consecutive days in August (August 3−6, 2019). Given wind directions from south−southeast (prevailing meteorology for Karnes County and Texas), and the 1-week duration of NOx emissions, these results suggest that MDA8 O_3 enhancements can be as high as 8−10 ppb in the areas lying north of the Eagle Ford Shale (such as San Antonio, and Bexar County) for several days during the peak ozone season.

Impact on Spatial and Temporal Extent of Ozone Exceedance. Figure 5 illustrates that some regions in the domain can experience higher MDA8 O_3 concentrations in Cases 2−4 compared to Case 1, while other regions show lower concentrations in Cases 2−4 than in Case 1. Understanding the spatial and temporal extent of these enhancements especially becomes important if ozone levels in these regions exceed regulatory standards such as the NAAQS. To assess the domain-wide impact and the daily evolution of ozone exceedances across the cases, the total geographical area within the domain exceeding a threshold MDA8 O_3 concentration of 60 ppb was calculated for Cases 1−4. The difference in this area between Cases 2−4 and Case 1 was computed and normalized by the area of Case 1. This normalized metric quantified the daily fractional change in domain area exceeding the 60 ppb MDA8 O_3 threshold in Cases 2−4, where NOx emissions from hydraulic fracturing are episodic and localized compared to Case 1, where these emissions are evenly distributed.

Table S5 shows the frequency distribution of differences in the geographical area exceeding a threshold of 60 ppbV of MDA8 O_3 concentrations between Cases 2−4 and Case 1. In Cases 2 and 3, where NOx emissions from hydraulic fracturing are solely allocated to fractured wells for durations of 1 and 2 weeks, the geographical area exceeding the 60 ppbV threshold

https://doi.org/10.1021/acsestair.4c00077
ACS EST Air 2025, 2, 130−140

of MDA8 O_3 was consistently equal to or larger than that predicted in Case 1 for all episode days. Specifically, for Case 3 with a 1 week emission duration, there were 40 days out of the total 213 episode days where the geographical area of exceedance (MDA8 O_3 > 60 ppb) was 20% more than the area predicted in Case 1. In Case 4, there is 1 day within the entire episode where the geographical area of exceedance is less than that of Case 1 area. This is likely due to high NOx emission rates (Table 2), resulting in lower MDA8 O_3 concentrations in those specific regions.

Table S6 presents similar results for differences in the total geographic time-integrated area of exceedance between Cases 2−4 and Case 1. The time integrated area quantifies changes in the spatial extent of ozone exceedance each hour and reflects the cumulative impact throughout the day. For Case 3 (1-week emission period), there were 35 days out of the total 213 episode days for which the time-integrated area was more than 20% of the Case 1 area. These findings suggest that detailed spatial and temporal allocation of NOx emissions from hydraulic fracturing leads to an increase in both the area where predicted ozone levels exceed a threshold of 60 ppb (spatial extent) and the duration of these exceedances (temporal extent).

Implications for Bexar County and San Antonio. In October 2022, the U.S. EPA reclassified San Antonio, Bexar County, from a "marginal" to a "moderate" level of nonattainment for the 2015 Ozone NAAQS.[24] To understand the impact of localized and transient NOx emissions from hydraulic fracturing on ozone formation, MDA8 O_3 concentrations were extracted for grid cells within the extent of Bexar County (shown in Figure S5A) for all four cases on all episode days. Figure 6 presents the maximum and minimum differences in these MDA8 O_3 concentrations between Cases 2−4 and Case 1 for August. Notably, for Case 3 (1 week emission duration), MDA8 O_3 concentrations consistently exceeded those of Case 1 by 5 ppb or more throughout August, indicating a strong and persistent impact of spatially and temporally allocated NOx emissions from hydraulic fracturing on ozone formation in Bexar County.

Out of the 436 wells fractured in Karnes County in 2019, approximately 44 wells were undergoing fracturing in August (assuming 1 week emission duration, Case 3). Most days in August observed more than 5 wells with fracturing activity (Figure S4), resulting in a persistent collective NOx emission rate of 3 tons per day or more. Moreover, half of the month experienced NOx emissions exceeding 5 tons per day (9 or more wells undergoing fracturing). Given that Karnes County frequently lies upwind of Bexar County, and ozone formation in these regions is predominantly NOx-limited, localized, and transient NOx emissions from hydraulic fracturing can impact the regional ozone formation in Bexar County.

Hourly predicted O_3 concentrations were also extracted for all four cases at the grid cell nearest to one of the Continuous Ambient Monitoring Stations (CAMS, 0023) in San Antonio. This station, situated in northwest San Antonio (Figure S6A), is located downwind of the Eagle Ford Shale with respect to the prevailing meteorology. Figure S6B compares the differences in hourly O_3 concentrations between Cases 2−4 and Case 1 for August. Like Bexar County, 1 h of O_3 concentrations near CAMS 0023 were also consistently 5 ppb higher for Case 3 (1 week duration) than Case 1. Low O_3 concentrations for Case 4 (2 day emission duration) suggest a potential VOC-limited regime due to high NOx emission rates. Nevertheless, these results also demonstrate that precise spatial and temporal allocation of NOx emissions from hydraulic fracturing in Karnes County results in increased predicted regional ozone formation near San Antonio. Performance evaluation at this monitoring station, along with four other CAMS[47] near San Antonio, is described in Section S6 of the SI.

Finally, Relative Response Factors (RRF) for ozone were calculated at five Continuous Ambient Monitoring Stations (CAMS) in San Antonio (Figure S6A). RRF is used to quantify the relative change in ozone concentrations between a baseline scenario and future scenarios with altered emissions and to demonstrate attainment/nonattainment at monitoring locations.[48,49]

Case 1, where NOx emissions from hydraulic fracturing were evenly distributed across Karnes County, served as the baseline scenario. Cases 2−4, where these emissions were distributed only to fractured wells for periods of 2 weeks, 1 week, and 2 days, respectively, served as the test case scenarios. RRF for ozone was calculated using two methodologies based on EPA guidance, as detailed in the SI.[48,50] Briefly, RRF at a monitor i was calculated as

$$\mathrm{RRF}_i = \frac{\text{mean of MDA8 } O_3 \text{ concentrations on selected days in test case}_i}{\text{mean of MDA8 } O_3 \text{ concentrations on selected days in case 1}_i}$$

Tables S7 and S8 in the SI present the RRF values derived from two methods for each of the three cases and five CAMS.

RRF for ozone is used alongside a Baseline Design Value (DVB) to calculate Future Design Values (DVF) and assess compliance with NAAQS at the monitoring locations. DVF at a monitoring station i is calculated as follows:

$$\text{Future Design Value (DVF)}_i = \mathrm{RRF}_i \times \text{Base Design Value (DVB)}_i$$

where DVB is the average of three design value periods centered on the baseline inventory year.[48] For this analysis, the baseline inventory year was 2019, and the three design value periods were 2017−2019, 2018−2020, and 2019−2021. If the calculated DVF exceeds the NAAQS for ozone (70 ppb) at a monitor, then the monitor is considered to be in nonattainment.[48]

Using an average DVB of 0.073 ppm for San Antonio and modeled RRF, DVFs were calculated for Cases 2−4 at all five CAMS (Tables S9 and S10).[51] DVFs for Cases 2−4 at all monitors were greater than or equal to 0.074 ppm (74 ppb), exceeding the NAAQS for ozone (70 ppb) and indicating potential larger magnitude of nonattainment at all five monitoring stations. Monitor-level design values were also available for CAMS 0023 (San Antonio, NW) and CAMS 0058 (Camp Bullis) for the three design value periods. The DVB at both stations was 0.072 ppm. Using this DVB and modeled RRF, DVFs at both stations was greater than or equal to 0.073 ppm for Cases 2−4 (Table S11).

The results presented in this work demonstrate that different allocation methods of NOx emissions from hydraulic fracturing, ranging from annual distribution to more episodic and local distribution, result in NOx emission rates due to hydraulic fracturing at individual sites varying by two to 3 orders of magnitude. UOGD activities like hydraulic fracturing contribute approximately 10% of total NOx emissions in the Eagle Ford Shale but occur only at selected well-sites and last only for 1−2 weeks prior to production. Accurate spatial and temporal allocation of their NOx emissions can lead to increased localized ozone formation in a NOx-limited region

https://doi.org/10.1021/acsestair.4c00077
ACS EST Air 2025, 2, 130−140

such as the Eagle Ford Shale. These results highlight the need for allocating NOx emissions from UOGD based on the nature and contribution of the source, especially in NOx-limited oil and gas production regions. If the assessment of hydraulic fracturing activities in similar regions is not accounting for the nature of emissions (i.e., spatial allocation and duration), then it might become difficult to identify mitigation strategies to reduce ozone concentrations below NAAQS and maintain attainment. Similar results might be expected for the drilling activity.

■ ASSOCIATED CONTENT

Supporting Information

The Supporting Information is available free of charge at https://pubs.acs.org/doi/10.1021/acsestair.4c00077.

Details of Case Study emission spatial and temporal distributions; maxima and minima of daily ozone concentrations; model performance evaluations; relative response factor for ozone; and future design values at monitoring locations (PDF)

■ AUTHOR INFORMATION

Corresponding Author

David T. Allen − *Center for Energy and Environmental Resources, The University of Texas at Austin, Austin, Texas 78758, United States;* orcid.org/0000-0001-6646-8755; Email: allen@che.utexas.edu

Authors

Mrinali Modi − *Center for Energy and Environmental Resources, The University of Texas at Austin, Austin, Texas 78758, United States;* orcid.org/0000-0002-9501-0513

Yosuke Kimura − *Center for Energy and Environmental Resources, The University of Texas at Austin, Austin, Texas 78758, United States*

Lea Hildebrandt Ruiz − *Center for Energy and Environmental Resources, The University of Texas at Austin, Austin, Texas 78758, United States;* orcid.org/0000-0001-8378-1882

Complete contact information is available at: https://pubs.acs.org/10.1021/acsestair.4c00077

Notes

The authors declare the following competing financial interest(s): D.T.A. and L.H.R serve on the Environmental Protection Agency's Science Advisory Board; in this role, they are paid Special Governmental Employees. L.H.Rs research is currently supported by the Texas Commission on Environmental Quality, the Health Effects Institute, and ExxonMobil. D.T.A.s research is currently supported by the National Science Foundation, the Department of Energy, the Texas Commission on Environmental Quality, the Collaboratory to Advance Methane Science, Chevron, ExxonMobil, Pioneer Natural Resources, and the Environmental Defense Fund. He has also worked on air quality projects that have been supported by oil and gas producers and the Environmental Defense Fund. D.T.A. has worked as a consultant for multiple companies, including British Petroleum, Cheniere, Eastern Research Group, KeyLogic, and SLR International.

■ ACKNOWLEDGMENTS

Research described in this article was conducted under contract to the Health Effects Institute (HEI), an organization jointly funded by the United States Environmental Protection Agency (EPA) (Contract No. 68HERC19D0010) and certain oil and natural gas companies. Although the research was produced with partial funding by EPA and industry, they have not been subject to their review, and therefore the research does not necessarily reflect the views of the Agency or the oil and natural gas industry, and no official endorsement by the Agency or the industry should be inferred. The authors also thank Professor Jeff Collett, Department of Atmospheric Science, Colorado State University, and Daniel Zimmerle, Director of Methane Emissions Program, Colorado State University, for their insights and valuable discussions.

■ REFERENCES

(1) Zhang, J. J.; Wei, Y.; Fang, Z. Ozone Pollution: A Major Health Hazard Worldwide. *Frontiers in Immunology* **2019**, *10*, 2518.

(2) Environmental Protection Agency Integrated Science Assessment for Ozone and Related Photochemical Oxidants. www.epa.gov/isa/integrated-science-assessment-isa-ozone-and-related-photochemical-oxidants (accessed 2024−12−15).

(3) Agathokleous, E.; Feng, Z.; Oksanen, E.; Sicard, P.; Wang, Q.; Saitanis, C. J.; Araminiene, V.; Blande, J. D.; Hayes, F.; Calatayud, V.; Domingos, M.; Veresoglou, S. D.; Peñuelas, J.; Wardle, D. A.; De Marco, A.; Li, Z.; Harmens, H.; Yuan, X.; Vitale, M.; Paoletti, E. Ozone Affects Plant, Insect, and Soil Microbial Communities: A Threat to Terrestrial Ecosystems and Biodiversity. *Science Advances* **2020**, *6*, No. eabc1176.

(4) Environmental Protection Agency. Criteria Air Pollutants NAAQS Table. https://www.epa.gov/criteria-air-pollutants/naaqs-table (accessed 2024−07−14).

(5) Environmental Protection Agency. Review of the Ozone National Ambient Air Quality Standards (40 CFR Part 50). Federal Register. December 31, 2020. https://www.govinfo.gov/content/pkg/FR-2020-12-31/pdf/2020-28871.pdf (accessed 2024−07−14).

(6) National Academies of Science, Engineering and Medicine *Rethinking the Ozone Problem in Urban and Regional Air Pollution*; National Academies Press, 1991. DOI: 10.17226/1889.

(7) HEI-Energy Research Committee. Potential Human Health Effects Associated with Unconventional and Gas Development: A Systematic Review of the Epidemiology Literature. Special Report 1. Boston, MA, 2019. https://www.heienergy.org/publication/potential-human-health-effects-associated-unconventional-oil-and-gas-development (accessed 2024−02−04).

(8) Dix, B.; de Bruin, J.; Roosenbrand, E.; Vlemmix, T.; Francoeur, C.; Gorchov-Negron, A.; McDonald, B.; Zhizhin, M.; Elvidge, C.; Veefkind, P.; Levelt, P.; de Gouw, J. Nitrogen Oxide Emissions from U.S. Oil and Gas Production: Recent Trends and Source Attribution. *Geophys. Res. Lett.* **2020**, *47* (1), No. e2019GL085866.

(9) Hecobian, A.; Clements, A. L.; Shonkwiler, K. B.; Zhou, Y.; MacDonald, L. P.; Hilliard, N.; Wells, B. L.; Bibeau, B.; Ham, J. M.; Pierce, J. R.; Collett, J. L. Air Toxics and Other Volatile Organic Compound Emissions from Unconventional Oil and Gas Development. *Environ. Sci. Technol. Lett.* **2019**, *6* (12), 720−726.

(10) Allen, D. T. Emissions from Oil and Gas Operations in the United States and Their Air Quality Implications. *J. Air Waste Manage Assoc* **2016**, *66* (6), 549−575.

(11) Moore, C. W.; Zielinska, B.; Pétron, G.; Jackson, R. B. Air Impacts of Increased Natural Gas Acquisition, Processing, and Use: A Critical Review. *Environ. Sci. Technol.* **2014**, *48*, 8349−8359.

(12) Cheadle, L. C.; Oltmans, S. J.; Pétron, G.; Schnell, R. C.; Mattson, E. J.; Herndon, S. C.; Thompson, A. M.; Blake, D. R.; McClure-Begley, A. Surface Ozone in the Colorado Northern Front Range and the Influence of Oil and Gas Development during FRAPPE/DISCOVER-AQ in Summer 2014. *Elementa* **2017**, *5*, 61.

(13) Helmig, D.; Thompson, C. R.; Evans, J.; Boylan, P.; Hueber, J.; Park, J. H. Highly Elevated Atmospheric Levels of Volatile Organic Compounds in the Uintah Basin, Utah. *Environ. Sci. Technol.* **2014**, *48* (9), 4707−4715.

(14) Schade, G. W.; Roest, G. Analysis of Non-Methane Hydrocarbon Data from a Monitoring Station Affected by Oil and Gas Development in the Eagle Ford Shale, Texas. *Elementa* **2016**, *4*, No. 000096.
(15) Swarthout, R. F.; Russo, R. S.; Zhou, Y.; Miller, B. M.; Mitchell, B.; Horsman, E.; Lipsky, E.; McCabe, D. C.; Baum, E.; Sive, B. C. Impact of Marcellus Shale Natural Gas Development in Southwest Pennsylvania on Volatile Organic Compound Emissions and Regional Air Quality. *Environ. Sci. Technol.* **2015**, *49* (5), 3175−3184.
(16) Dix, B.; Francoeur, C.; Li, M.; Serrano-Calvo, R.; Levelt, P. F.; Veefkind, J. P.; McDonald, B. C.; de Gouw, J. Quantifying NOx Emissions from U.S. Oil and Gas Production Regions Using TROPOMI NO2. *ACS Earth Space Chem.* **2022**, *6* (2), 403−414.
(17) Majid, A.; Val Martin, M.; Lamsal, L. N.; Duncan, B. N. A Decade of Changes in Nitrogen Oxides over Regions of Oil and Natural Gas Activity in the United States. *Elementa* **2017**, *5*, 76.
(18) Helmig, D. Air Quality Impacts from Oil and Natural Gas Development in Colorado. *Elementa* **2020**, *8*, 4.
(19) U.S. Energy Information Administration. Tight oil production estimates by play. https://www.eia.gov/petroleum/data.php (accessed 2023−10−17).
(20) U.S. Energy Information Administration. Dry shale gas production estimates by play. https://www.eia.gov/naturalgas/data.php#production (accessed 2023−10−17).
(21) Railroad Commission of Texas. Eagle Ford Shale. https://www.rrc.state.tx.us/oil-and-gas/major-oil-and-gas-formations/eagle-ford-shale/ (accessed 2023−03−13).
(22) U.S. Census Bureau, City and Town Population Totals 2020−2022. https://www.census.gov/data/tables/time-series/demo/popest/2020s-total-cities-and-towns.html (accessed 2023−10−09).
(23) Pacsi, A. P.; Kimura, Y.; McGaughey, G.; McDonald-Buller, E. C.; Allen, D. T. Regional Ozone Impacts of Increased Natural Gas Use in the Texas Power Sector and Development in the Eagle Ford Shale. *Environ. Sci. Technol.* **2015**, *49* (6), 3966−3973.
(24) Texas Commission on Environmental Quality. San Antonio: Ozone History. https://www.tceq.texas.gov/airquality/sip/san/san-ozone-history (accessed 2023−10−18).
(25) Wiedinmyer, C.; Guenther, A.; Estes, M.; Strange, I. W.; Yarwood, G.; Allen, D. T. A Land Use Database and Examples of Biogenic Isoprene Emission Estimates for the State of Texas, USA. *Atmos. Environ.* **2001**, *35* (36), 6465−6477.
(26) Yu, H.; Guenther, A.; Gu, D.; Warneke, C.; Geron, C.; Goldstein, A.; Graus, M.; Karl, T.; Kaser, L.; Misztal, P.; Yuan, B. Airborne Measurements of Isoprene and Monoterpene Emissions from Southeastern U.S. Forests. *Sci. Total Environ.* **2017**, *595*, 149−158.
(27) Anderson, D. C.; Pavelec, J.; Daube, C.; Herndon, S. C.; Knighton, W. B.; Lerner, B. M.; Roscioli, J. R.; Yacovitch, T. I.; Wood, E. C. Characterization of Ozone Production in San Antonio, Texas, Using Measurements of Total Peroxy Radicals. *Atmos Chem. Phys.* **2019**, *19* (5), 2845−2860.
(28) Pozzer, A.; Schultz, M. G.; Helmig, D. Impact of U.S. Oil and Natural Gas Emission Increases on Surface Ozone Is Most Pronounced in the Central United States. *Environ. Sci. Technol.* **2020**, *54* (19), 12423−12433.
(29) Roohani, Y. H.; Roy, A. A.; Heo, J.; Robinson, A. L.; Adams, P. J. Impact of Natural Gas Development in the Marcellus and Utica Shales on Regional Ozone and Fine Particulate Matter Levels. *Atmos. Environ.* **2017**, *155*, 11−20.
(30) Pacsi, A. P.; Alhajeri, N. S.; Zavala-Araiza, D.; Webster, M. D.; Allen, D. T. Regional Air Quality Impacts of Increased Natural Gas Production and Use in Texas. *Environ. Sci. Technol.* **2013**, *47* (7), 3521−3527.
(31) U.S. Environmental Protection Agency. 2020 National Emissions Inventory (NEI). https://www.epa.gov/air-emissions-inventories/2020-national-emissions-inventory-nei-data (accessed 2023−10−18).
(32) EPA Nonpoint Oil and Gas Emissions Estimation Tool V3, 2020. https://gaftp.epa.gov/Air/nei/2020/doc/supporting_data/nonpoint/oilgas/OIL_GAS_TOOL_v1.3/ (accessed 2023−01−31).
(33) U.S. Environmental Protection Agency. Compressor Starts. https://www.epa.gov/natural-gas-star-program/compressor-starts (accessed 2024−01−20).
(34) ConocoPhillips. Drilling and Extraction. https://alaska.conocophillips.com/what-we-do/oil-production/drilling-extraction/ (accessed 2024−07−15).
(35) Coloradans for Responsible Energy Development (CRED). How Long Does Fracking Last? https://www.cred.org/how-long-does-fracking-last/ (accessed 2024−07−15).
(36) Independent Petroleum Association of America. Hydraulic Fracturing. https://www.ipaa.org/fracking/ (accessed 2024−07−15).
(37) Mansfield Texas. Gas Well Drilling Process. https://www.mansfieldtexas.gov/356/Drilling-Process (accessed 2024−07−15).
(38) Pan, D.; Zhang, W.; Zhou, Y.; Ku, I.-T.; Kim, S.; Zimmerle, Z.; Duggan, J.; Rimelman, E.; McKenzie, L. M.; Finewax, Z.; Rickly, P. S.; Allen, D.; Hildebrandt Ruiz, L.; Collett, J. L. An Emission Model for Volatile Organic Compounds from Unconventional Oil and Gas Development. *American Geophysical Union Annual Meeting*, 2024, Washington D.C., Paper Number A23B-1955.
(39) Railroad Commission of Texas. Drilling Permits Data. https://www.rrc.texas.gov/resource-center/data-visualization/oil-gas-data-visualization/drilling-permits/ (accessed 2022−10−12).
(40) Railroad Commission of Texas. Oil and Gas Production Data Query. http://webapps.rrc.texas.gov/PDQ/generalReportAction.do (accessed 2022−10−12).
(41) Texas Commission on Environmental Quality. Texas Air Quality Modeling - Files and Information (2019 Platform). https://www.tceq.texas.gov/airquality/airmod/data/tx2019 (accessed 2023−10−19).
(42) Railroad Commission of Texas Online System. Oil and Gas Completions Completions Query. https://webapps.rrc.texas.gov/CMPL/publicHomeAction.do (accessed 2024−03−09).
(43) Ramboll. www.environcorp.com.
(44) Ramboll. User's Guide Comprehensive Air Quality Model with Extensions. https://www.camx.com/Files/CAMxUsersGuide_v7.20.pdf (accessed 2024−12−15).
(45) U.S. Environmental Protection Agency. Ozone National Ambient Air Quality Standards (NAAQS). https://www.epa.gov/ground-level-ozone-pollution/ozone-national-ambient-air-quality-standards-naaqs (accessed 2024−01−21).
(46) Texas Commission on Environmental Quality. San Antonio Northwest C23. https://www.tceq.texas.gov/cgi-bin/compliance/monops/site_photo.pl?cams=23 (accessed 2024−01−21).
(47) Texas Commission on Environmental Quality. Air Monitoring Sites. https://www.tceq.texas.gov/airquality/monops/sites (accessed 2024−09−22).
(48) U.S. Environmental Protection Agency. Guidance on the Use of Models and Other Analyses for Demonstrating Attainment of Air Quality Goals for Ozone, PM 2.5, and Regional Haze, EPA454/B-07-002, April 2007.
(49) Wang, L.; Thompson, T.; Mcdonald-Buller, E. C.; Webb, A.; Allen, D. T. Photochemical Modeling of Emissions Trading of Highly Reactive Volatile Organic Compounds in Houston, Texas. 1. Reactivity Based Trading and Potential for Ozone Hot Spot Formation. *Environ. Sci. Technol.* **2007**, *41*, 2095−2102.
(50) Foley, K. M.; Dolwick, P.; Hogrefe, C.; Simon, H.; Timin, B.; Possiel, N. Dynamic Evaluation of CMAQ Part II: Evaluation of Relative Response Factor Metrics for Ozone Attainment Demonstrations. *Atmos. Environ.* **2015**, *103*, 188−195.
(51) U.S. Environmental Protection Agency. Air Quality Design Values. https://www.epa.gov/air-trends/air-quality-design-values (accessed 2024−09−22).

https://doi.org/10.1021/acsestair.4c00077
ACS EST Air 2025, 2, 130−140